

Article

# Evaluation of SMAP-Enhanced Products Using Upscaled Soil Moisture Data Based on Random Forest Regression: A Case Study of the Qinghai–Tibet Plateau, China

Jia Chen <sup>1</sup> , Fengmin Hu <sup>2</sup>, Junjie Li <sup>1</sup>, Yijia Xie <sup>1</sup>, Wen Zhang <sup>1</sup>, Changqing Huang <sup>1</sup> and Lingkui Meng <sup>1,\*</sup>

<sup>1</sup> School of Remote Sensing and Information Engineering, Wuhan University, Wuhan 430079, China; whuchenjia@whu.edu.cn (J.C.); junjieli@whu.edu.cn (J.L.); 2017302590075@whu.edu.cn (Y.X.); wen\_zhang@whu.edu.cn (W.Z.); huangcq@whu.edu.cn (C.H.)

<sup>2</sup> College of Surveying and Geo-Informatics, North China University of Water Resources and Electric Power, Zhengzhou 450045, China; hufengmin@ncwu.edu.cn

\* Correspondence: lkmeng@whu.edu.cn; Tel.: +86-159-2706-6565

**Abstract:** The evaluation of satellite soil moisture is a big challenge owing to the large spatial mismatch between pixel-based satellite soil moisture products and point-based in situ measurements. Upscaling in situ measurements to obtain the “true value” of soil moisture content at the satellite grid/footprint scale can make up for the scale difference and improve the validation. Many existing upscaling methods have strict requirements regarding the spatial distribution and quantity of soil moisture sensors. However, in reality, soil-moisture-monitoring networks are commonly sparse with low sensor density, which increases the difficulty of obtaining accurate upscaled soil moisture data and limits the validation of satellite products. For this reason, this paper proposes a scheme to upscale in situ measurements using five machine learning methods along with Landsat 8 datasets and DEM data to validate the accuracy of a SMAP-enhanced passive soil moisture product for a sparse network on the Qinghai–Tibet Plateau. The proposed scheme realizes the upscaling of in situ soil moisture data to the pixel scale (30 m × 30 m) and then to the coarse grid scale (9 km × 9 km) by using multi-source remote sensing data as the bridge of scale conversion. The long-time SMAP SM products since April 2015 on the Qinghai–Tibet Plateau were validated based on upscaled soil moisture data. The results show that (1) random forest regression performs the best, and the upscaled soil moisture data reflect the region-average soil moisture conditions that can be used for evaluating SMAP data; (2) the SMAP product meets its scientific measurement requirements; and (3) the SMAP product generally underestimates the soil moisture in the study area.

**Keywords:** soil moisture; SMAP; evaluation; sparse ground-based sites; upscaling; random forest regression



**Citation:** Chen, J.; Hu, F.; Li, J.; Xie, Y.; Zhang, W.; Huang, C.; Meng, L. Evaluation of SMAP-Enhanced Products Using Upscaled Soil Moisture Data Based on Random Forest Regression: A Case Study of the Qinghai–Tibet Plateau, China. *ISPRS Int. J. Geo-Inf.* **2023**, *12*, 281. <https://doi.org/10.3390/ijgi12070281>

Academic Editors: Diego González-Aguilera, Pablo Rodríguez-Gonzálvez and Wolfgang Kainz

Received: 28 April 2023

Revised: 28 June 2023

Accepted: 11 July 2023

Published: 15 July 2023



**Copyright:** © 2023 by the authors. Licensee MDPI, Basel, Switzerland. This article is an open access article distributed under the terms and conditions of the Creative Commons Attribution (CC BY) license (<https://creativecommons.org/licenses/by/4.0/>).

## 1. Introduction

Soil moisture (SM) is a key element in geoscience research, reflecting the moisture status of the land surface and playing a crucial role in regulating global water and energy cycles [1–3]. High-quality soil moisture information is essential for flood/drought prediction and warning, agricultural monitoring, weather forecasting, and other fields [4–6]. For a long time, it has been difficult to obtain large-scale soil moisture data due to the expensive installation and maintenance costs of traditional ground-based soil-moisture-monitoring systems [7,8]. In recent years, continuous advances in remote sensing technology have made worldwide soil moisture measurements possible [9,10].

Satellite SM products need to be verified with high-precision in situ measurements to assess their accuracy [11,12]. However, it is unreasonable to compare pixel-based satellite soil moisture products and point-based in situ measurements directly, owing to the large spatial mismatch between them [13,14]. Therefore, upscaling becomes a very important

step during validation. It converts the data scale from the small scale to the large scale, thus providing the reference SM values at the satellite scale for the validation of satellite SM products [15]. There are several upscaling methods based on in situ measurements: (1) simple averaging, which directly calculates the arithmetic mean of all in situ measurements within the satellite grid and regards it as the “true value” of the grid [4,16,17]; (2) Kriging, a traditional geostatistical method, which uses the spatially correlated structure of in situ measurements among sites to estimate soil moisture of the whole region [18,19]; and (3) the model-driven method, which simulates the spatial pattern of soil moisture by building a land surface model [20–23]. Due to the strong spatial heterogeneity of soil moisture, many methods need a certain number of SM sensors to ensure that their upscaled soil moisture data can accurately reflect the real soil moisture conditions at large scales [24,25]. However, a large number of available soil moisture monitoring networks around the world have a low density of observation sites; in some cases, only one site is distributed within a single satellite grid [15,26]. For such sparse ground-based observations, the upscaled soil moisture data based only on a limited number of in situ measurements are not representative. Therefore, extra information is required to support upscaling, and higher-resolution remote sensing images become a great option [27–29]. Clewley et al. [30] used satellite products derived from Landsat data and DEM to carry out upscaling experiments. Qin et al. [24] and Kang et al. [26] used MODIS-derived apparent thermal inertia to scale up in situ measurements. These previous studies showed that introducing remote sensing data or its derived data as auxiliary information into the upscaling can improve the upscaling accuracy effectively.

Currently, the soil moisture active passive (SMAP) satellite maps land surface soil moisture and detects soil freeze–thaw states at a global scale through the collaboration of its synthetic aperture radar and radiometer [31]. It began operation in April 2015, but, unfortunately, its radar stopped working after July 2015, and now only the radiometer is operating. It publicly provides SM products with 36 km and 9 km grid cells [32]. To date, SMAP products have undergone extensive validations in data-rich regions in the United States, Europe, and China [10,14,33–36], while much less work is conducted in areas with sparse ground-based observations.

The Qinghai–Tibet Plateau is the origin of many large rivers in Asia [37,38], and it can directly drive climate change in its surrounding areas through atmospheric and hydrological processes [39,40]. Obtaining high-quality and large-scale soil moisture data on the Tibetan Plateau is of great importance. The SM sensors in the Ngari region of the Qinghai–Tibet Plateau are very sparse, and it is challenging to evaluate the 9 km SMAP SM products using reliable upscaled SM data. In this paper, we introduce multi-source remote sensing auxiliary information with a spatial resolution of 30 m to conduct upscaling experiments on the Ngari network, aiming to find an appropriate upscaling method for sparse soil moisture networks, obtain reliable upscaled soil moisture time series, and validate long-term SMAP products. In addition, while most previous satellite product validations have been based on short-term data (1–3 years) [39,41], this paper utilizes multi-source remote sensing data and the upscaling method to obtain reference SM values from 2013 to 2021, enabling the validation of SMAP products over a longer time series (since 2015). The format of this paper is as follows. Section 2 introduces the research data. Section 3 describes the upscaling strategy and evaluation metrics. Sections 4 and 5 give the results and discussion, respectively. Finally, Section 6 presents the conclusions of this study.

## 2. Study Data

### 2.1. SMAP SM Product

The soil moisture active passive (SMAP) mission carries an L-band radiometer and an L-band synthetic aperture radar to detect global land surface soil moisture and freeze–thaw states. The radiometer and radar can map soil moisture at a spatial resolution of 36 km and freeze–thaw conditions at a spatial resolution of 3 km, respectively, while they can cooperate to produce 9 km soil moisture products. After the radar stopped working in July 2015, the

SMAP mission remained committed to providing high-resolution observations, even with only the passive radiometer working [32]. SPL3SMP\_E is a SMAP-enhanced Level-3 daily composite SM product derived from the Backus–Gilbert interpolated radiometer brightness temperature measurements that are posted on the 9 km EASE-Grid 2.0. It can provide daily SM estimates of the upper 0–5 cm soil layer across the global land surface, and more details can be found in SMAP (<https://smap.jpl.nasa.gov/>, accessed on 17 February 2022). In this paper, we chose the SPL3SMP\_E products (V4) in the Ngari region from April 2015 to December 2021 for evaluation.

## 2.2. In Situ Observations

The Ngari soil moisture and soil temperature monitoring network is located in the western Qinghai–Tibet Plateau in a cold arid environment [42]. In this area, the surface land cover is mainly desert and alpine meadow, and the overall soil moisture content is low. Since the network was established in 2008, its sites have continuously measured soil moisture at various depths (5–80 cm) at 15 min intervals. During this period, some sites were damaged, and several new sites were added. At present, there are 13 sites that can provide long-term normal observation data (SQ02, SQ03, SQ06, SQ07, SQ08, SQ10, SQ11, SQ14, SQ17, SQ18, SQ19, SQ20, SQ21), which are distributed in an area of about 45 km × 45 km. More information can be read in [43]. Figure 1 shows the distribution of normal SM sensors in the study area and outlines the specific validation area of the SMAP SM product in this paper with a pink frame, which marks the corresponding 9 km EASE-2 grid. It is clear that the SM sensors of the Ngari network are sparse, and there are often only one or even no effective sites in a single 9 km EASE-2 grid. In this paper, we used in situ measurements at 5 cm from March 2013 to September 2019.

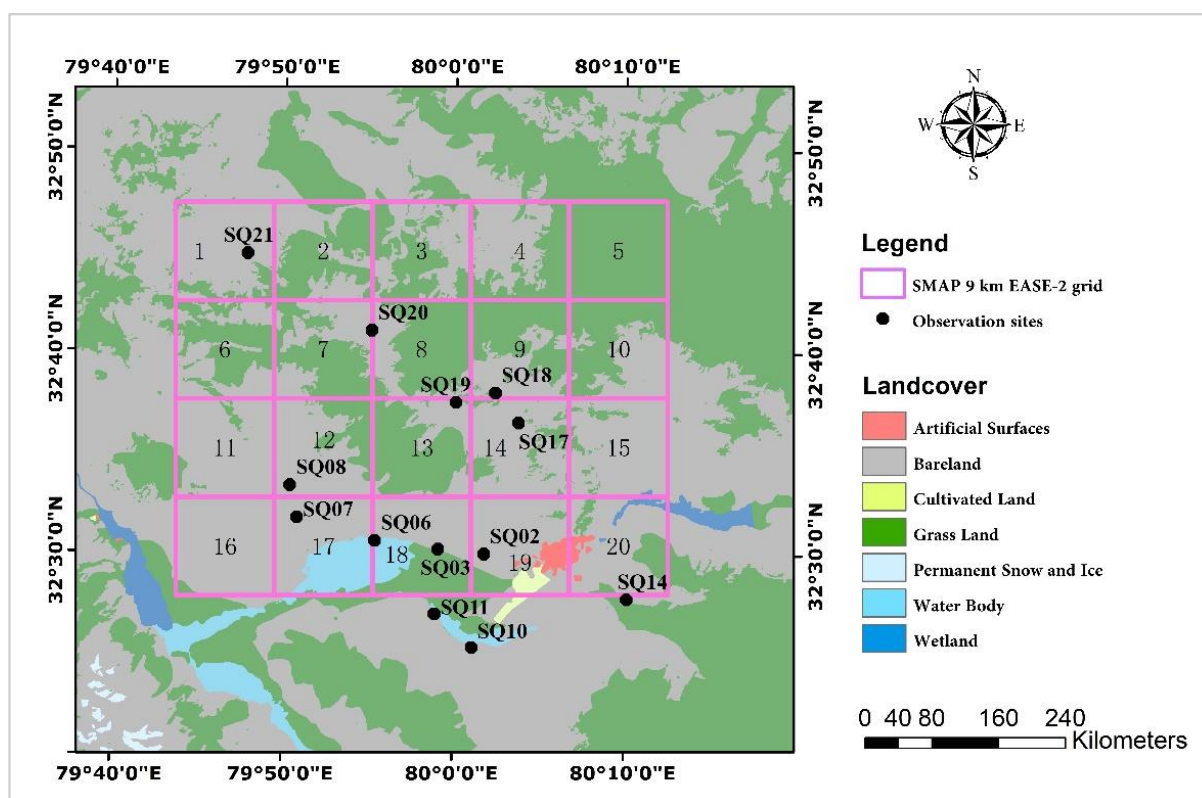


**Figure 1.** Distribution of the Ngari network observation sites on the Qinghai–Tibet Plateau, with the background indicating the land cover conditions (from GlobeLand30, accessed on 21 March 2022). The SMAP validation area is delineated using the 9 km EASE-2 grid and labeled with serial numbers 1–20.

### 2.3. Ancillary Datasets

The remote sensing auxiliary data used in this study were taken from Landsat 8 satellite observation data and an ASTER GDEM digital elevation model, both with a spatial resolution of 30 m.

#### (1) Landsat 8 satellite observation

Landsat 8, one of the Landsat satellites, was jointly developed by NASA and the USGS and launched in February 2013. Landsat 8 is equipped with two payloads, a thermal infrared sensor (TIRS) and an operational land imager (OLI), to provide satellite observation data of the global land surface with spatial resolutions of 15 m, 30 m, and 100 m. More details can be found in Landsat Science (<https://landsat.gsfc.nasa.gov/>, accessed on 22 February 2022). In this paper, the land surface reflectance of the OLI sensor from March 2013 to December 2021 and the derived normalized difference vegetation index (NDVI) information were used. Among them, the data from March 2013 to September 2019 were used to build the upscaling model together with the in situ measurement, and the data from March 2013 to December 2021 were upscaled using the model to validate the SMAP products.

#### (2) Digital Elevation Model

The advanced spaceborne thermal emission and reflection radiometer global digital elevation model (ASTER GDEM) is a digital elevation product jointly developed and released by NASA and METI. Its products are generated from stereo images collected by the ASTER sensor with a spatial resolution of 30 m. They are able to cover all land between 83° N and 83° S latitude, which is about 99% of the world's land area. More details can be found in ASTER (<https://asterweb.jpl.nasa.gov/>, accessed on 21 March 2022). This study used the ASTER GDEM V3 elevation data released in August 2019 and obtained the slope and aspect of the terrain parameters for upscaling research.

## 3. Method

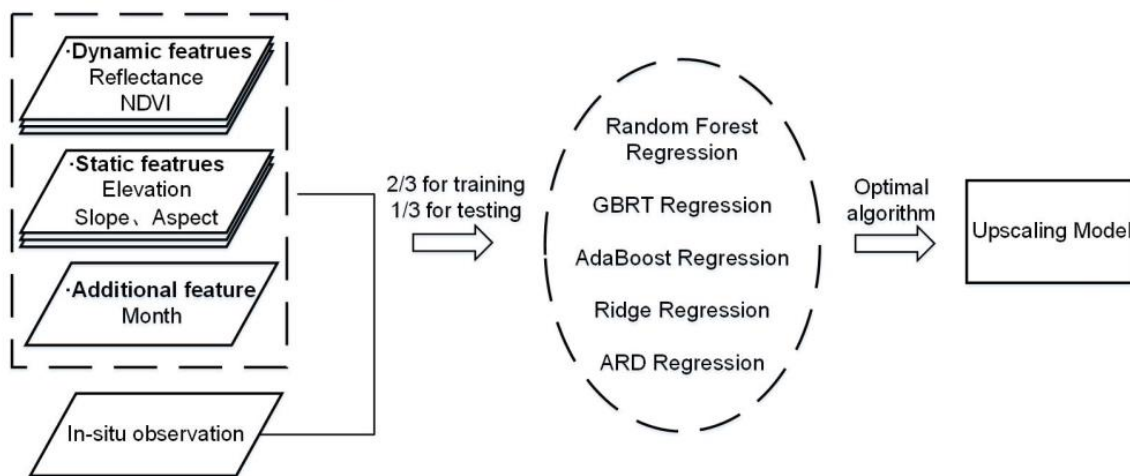
### 3.1. Upscaling Strategy

In order to make up for the huge scale difference between the satellite observations and the in situ measurements, the satellite SM product validation needs to scale up the in situ measurements to provide the reference SM value of the grid scale. Generally, when a sufficient number of valid in situ measurements are available for an area, their average value can be considered as the true value of the soil moisture in the area. However, in reality, many soil-moisture-monitoring network sensors are not dense enough, including the Ngari network. It is challenging to validate satellite SM products based on sparse observations because the area-average soil moisture value obtained from limited field measurements is not representative. The key to solving this problem is to supplement additional effective soil moisture information to make up for the insufficiency of in situ measurements, so as to ensure that the average soil moisture obtained can reflect the true soil moisture conditions. The higher-resolution remote sensing image is a good choice of auxiliary data for the following reasons:

- Satellite images are reliable auxiliary data sources, which have long-term time series and are easy to access;
- Satellite images cover a wide range, which can make up for the deficiency of in situ measurements to a certain extent;
- Satellite images are spatially continuous and uniformly sampled, which can effectively capture the spatial heterogeneity of soil moisture, and thereby reflect the soil moisture status more accurately [27,28];
- Their high resolution means that each pixel is purer than those of coarse-resolution images, and therefore the spatial difference between the pixel measurement and point measurement is not too large.

In this study, we assumed that a single in situ measurement can represent the soil moisture situation within about 30 m of the site, and based on this assumption, we used 30 m multi-source remote sensing images as the scale conversion bridge. Our upscaling strategy can be divided into the following two steps: the first step is to construct an upscaling model by fitting the in situ measurements to the remote sensing images, and then use the model to estimate the 30 m soil moisture values over the entire study area. In the second step, we average the valid 30 m soil moisture estimates corresponding to each satellite grid to obtain the reference 9 km soil moisture values. This method fully considers the spatial heterogeneity of soil moisture and the spatial representation capability of in situ measurements, and the whole upscaling process is shown in Figure 2.

### Phase I : Build upscaling model



### Phase II : Estimate soil moisture at 9 km

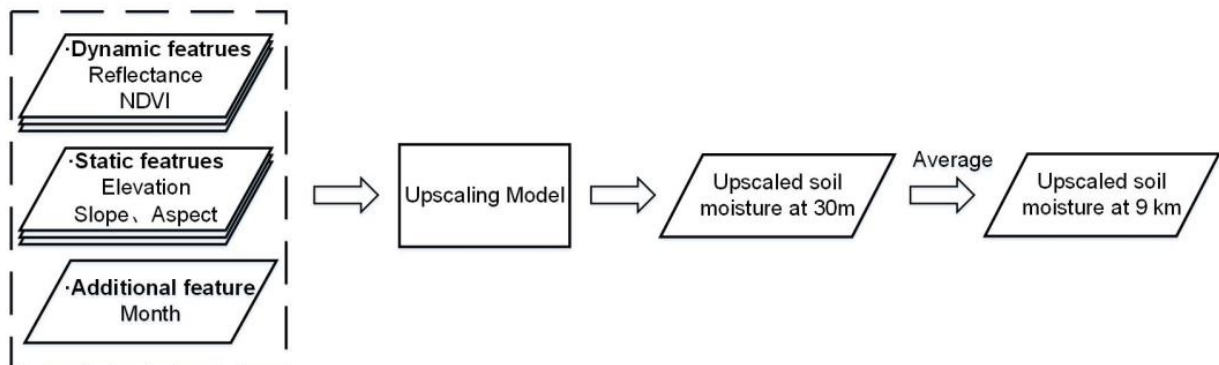


**Figure 2.** Schematic diagram of the methodology.

Considering that soil moisture is affected by terrain, vegetation cover, soil properties, and other factors [15,44], we chose Landsat 8 surface reflectance, ASTER GDEM, and their derived data as auxiliary information. These auxiliary data can be divided into two categories: static features and dynamic features. Static features include elevation, slope, and aspect, which are closely related to soil moisture but remain constant over time. Dynamic features include seven bands of land surface reflectance and NDVI, which change with time and can dynamically reflect changes in soil moisture. In addition, noting the obvious seasonal variation in soil moisture, we also included the month in the upscaling experiments. All auxiliary data were divided into two datasets; one was used to build up the upscaling models together with the in situ measurements, and the other was used to obtain the 9 km soil moisture estimates for the validation of the SMAP products. It should be noted that, to ensure the temporal consistency of the data, we used daily-averaged in situ

measurements consistent with the Landsat product dates for the upscaling experiments. The integration of in situ measurements from 13 soil moisture sites with multi-source remote sensing data from 2013 to 2019 yielded 2054 sets of data. In order to ensure the model's accuracy, we removed abnormal values in the in-situ measurements and filtered out cloud-contaminated remote sensing data. Consequently, we obtained a final sample dataset consisting of 756 sets of data. The auxiliary data used were of various types and large quantities. In order to properly simulate the complex relationship between in situ measurements and various input features, we preferentially selected the random forest regression (RFR) [45] algorithm for the upscale experiment, which has performed well in previous scale conversion experiments [6,30]. In addition, we selected four other machine learning algorithms: gradient boosting regression tree (GBRT) regression [46], AdaBoost regression [47], ridge regression (RR) [48], and automatic relevance determination (ARD) regression for comparative experiments. Compared with some other traditional regression algorithms, these selected algorithms are able to process large batches of data quickly and efficiently, and they can model complex nonlinear systems [28,49,50]. During the experiment, 2/3 of the study data were randomly selected for training, and the remaining 1/3 was used to test the model. Furthermore, the upscaled soil moisture data were verified by in situ measurements.

### 3.2. Validation Metrics

In this paper, four statistical indicators [51,52], the correlation coefficient ( $R$ , *bias*, root mean square error ( $RMSE$ ), and unbiased root mean square error ( $ubRMSE$ ), are used to comprehensively evaluate upscaled soil moisture and satellite soil moisture products.  $R$  represents the time correlation between two datasets, and the closer the  $R$  value is to 1, the more similar their changing trends are. *Bias* describes the error; a positive value indicates an underestimation, while a negative value indicates an overestimation.  $RMSE$  reflects the degree of deviation between two datasets, and  $ubRMSE$  represents the average error after removing the mean deviation. The smaller the values of these two metrics, the more similar the two datasets are. The calculation formulae of the evaluation indices are as follows:

$$R = \frac{\sum_{i=1}^N (SM_i^x - \overline{SM}^x) (SM_i^y - \overline{SM}^y)}{\sqrt{\sum_{i=1}^N (SM_i^x - \overline{SM}^x)^2} \sqrt{\sum_{i=1}^N (SM_i^y - \overline{SM}^y)^2}} \quad (1)$$

$$Bias = \frac{1}{N} \sum_{i=1}^N (SM_i^y - SM_i^x) \quad (2)$$

$$RMSE = \sqrt{\frac{1}{N} \sum_{i=1}^N (SM_i^y - SM_i^x)^2} \quad (3)$$

$$ubRMSE = \sqrt{RMSE^2 - Bias^2} \quad (4)$$

According to the upscaling strategy, upscaling results need to be validated using in situ measurements, while the SMAP products need to be evaluated using upscaled soil moisture data at the 9 km scale. Therefore, when evaluating the upscaling results,  $SM^x$  represents the upscaled soil moisture data,  $SM^y$  represents the in situ measurements, and  $N$  represents the number of samples involved in the calculation; when evaluating SMAP products,  $SM^x$  represents the satellite-observed soil moisture,  $SM^y$  represents the upscaled soil moisture at the 9 km scale, and  $N$  represents the number of samples involved in the calculation. It should be noted that the SMAP baseline requirement is that the  $ubRMSE$  of the soil moisture in the top 5 cm depth of soil must be less than  $0.04 \text{ m}^3/\text{m}^3$ .

## 4. Results

### 4.1. Evaluation of the Upscaling Result

Five upscaling algorithms were run on in situ data and auxiliary data to construct the upscaling models. We trained upscaling models with two-thirds of the data from March 2013 to December 2019—since the Landsat 8 data are available—and verified the performance of the five models using the remaining data. The evaluation results are shown in Table 1. Among the five algorithms, the RFR algorithm performed the best with the lowest *ubRMSE* ( $0.029 \text{ m}^3/\text{m}^3$ ) and *RMSE* ( $0.029 \text{ m}^3/\text{m}^3$ ), the smallest *bias* ( $-0.002 \text{ m}^3/\text{m}^3$ ), and the highest *R* (0.826), which shows that the average error between the in situ measurements and the upscaled soil moisture is small, and they have a high degree of correlation and similar change trends. The GBRT algorithm was slightly inferior to the RFR algorithm, but its performance was still surprising. As for the other three algorithms, they have larger *ubRMSE* and *RMSE*, as well as a smaller *R*, indicating that their performance was worse than the RFR algorithm and the GBRT algorithm.

**Table 1.** Evaluation metrics of five upscaling algorithms. The best and worst values in each column are highlighted in bold underline and bold, respectively.

Upscaling Algorithm	<i>ubRMSE</i> ( $\text{m}^3/\text{m}^3$ )	<i>RMSE</i> ( $\text{m}^3/\text{m}^3$ )	<i>Bias</i> ( $\text{m}^3/\text{m}^3$ )	<i>R</i>
Random Forest Regression	<b><u>0.029</u></b>	<b><u>0.029</u></b>	<b><u>-0.002</u></b>	<b><u>0.826</u></b>
GBRT Regression	0.03	0.03	-0.004	0.809
AdaBoost Regression	0.031	0.036	<b>-0.018</b>	0.781
Ridge Regression	0.036	0.036	-0.004	0.697
ARD Regression	<b><u>0.039</u></b>	<b><u>0.038</u></b>	-0.004	<b><u>0.665</u></b>

Figure 3 plots the time series of in situ measurements and the upscaled soil moisture estimated by the five upscaling models. It shows that the estimates of soil moisture based on the RFR model are similar to the in situ measurements, showing a good upscaling effect. The estimates based on the GBRT model are also very close to the in situ measurements, but there are obvious deviations in a few cases. The upscaling effect of the other three models is not ideal. Among them, the AdaBoost model always overestimated the soil moisture, and the RR and ARD models were unstable during upscaling. By comparing the five upscaling algorithms, it was found that the RFR can accurately simulate the complex relationship between in situ measurements and various features, and its model has an ideal upscaling effect.

Figure 4 shows scatter plots between in situ SM and the 30 m SM estimates based on the RFR upscaling model. The *R* values of the SM estimates and the in situ measurements at all sites are above 0.7, and most of them are between 0.8 and 1, showing a good correlation. In addition, the *bias*, *RMSE*, and *ubRMSE* are all small, and no abnormal results are observed. Overall, the RFR upscaling model runs stably and performs well at upscaling.

To sum up, the upscaling model trained by the RFR algorithm can accurately simulate the complex nonlinear relationship between multi-source auxiliary data and in situ measurements, and its soil moisture estimates can be used as valid supplementary data.

### 4.2. Soil Moisture Based on Upscaling

As discussed above, we used the RFR upscaling model to obtain soil moisture data at the 30 m scale across the entire study area. Figure 5 shows the estimated soil moisture at the 30 m scale in Ngari, and the white grids in the figure represent clouds, which are regarded as invalid data. It reveals that the upscaled soil moisture is highest in the iceberg and lake area, and higher in the vegetation area than in the bare land area, which is consistent with the actual situation.

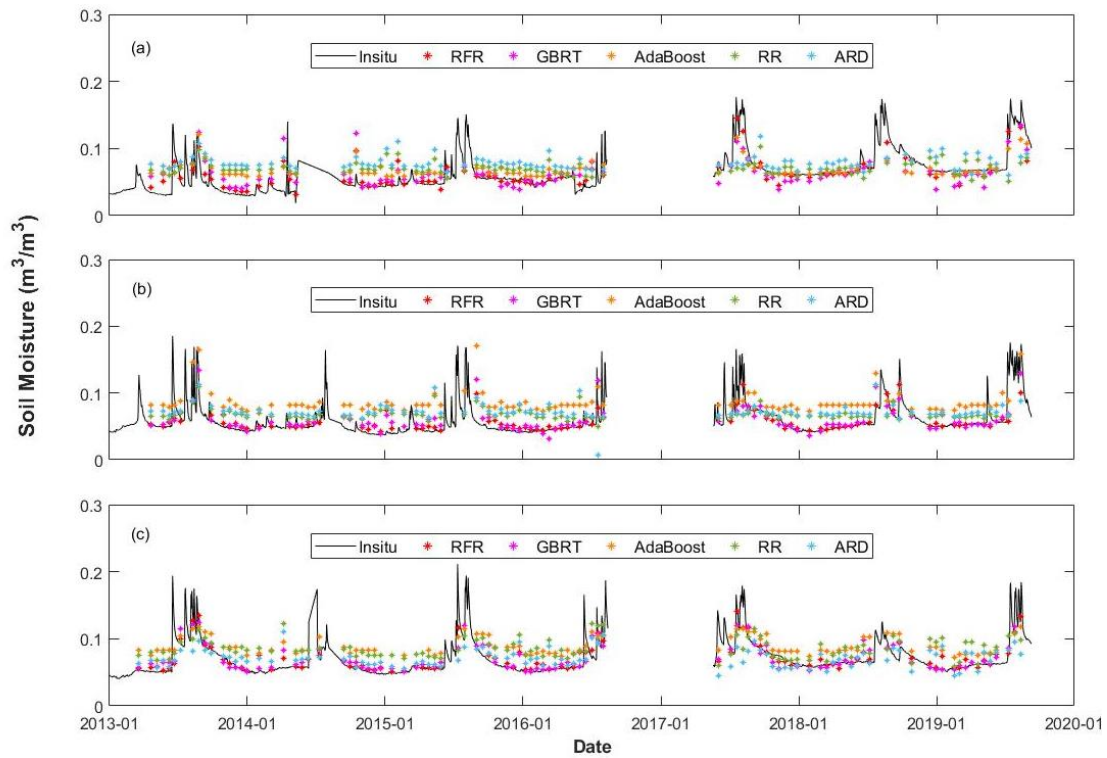


Figure 3. Comparison between in situ measurements and SM estimates based on five models (In situ measurements from September 2016 to April 2017 are missing). (a) SQ02, (b) SQ03, (c) SQ14.

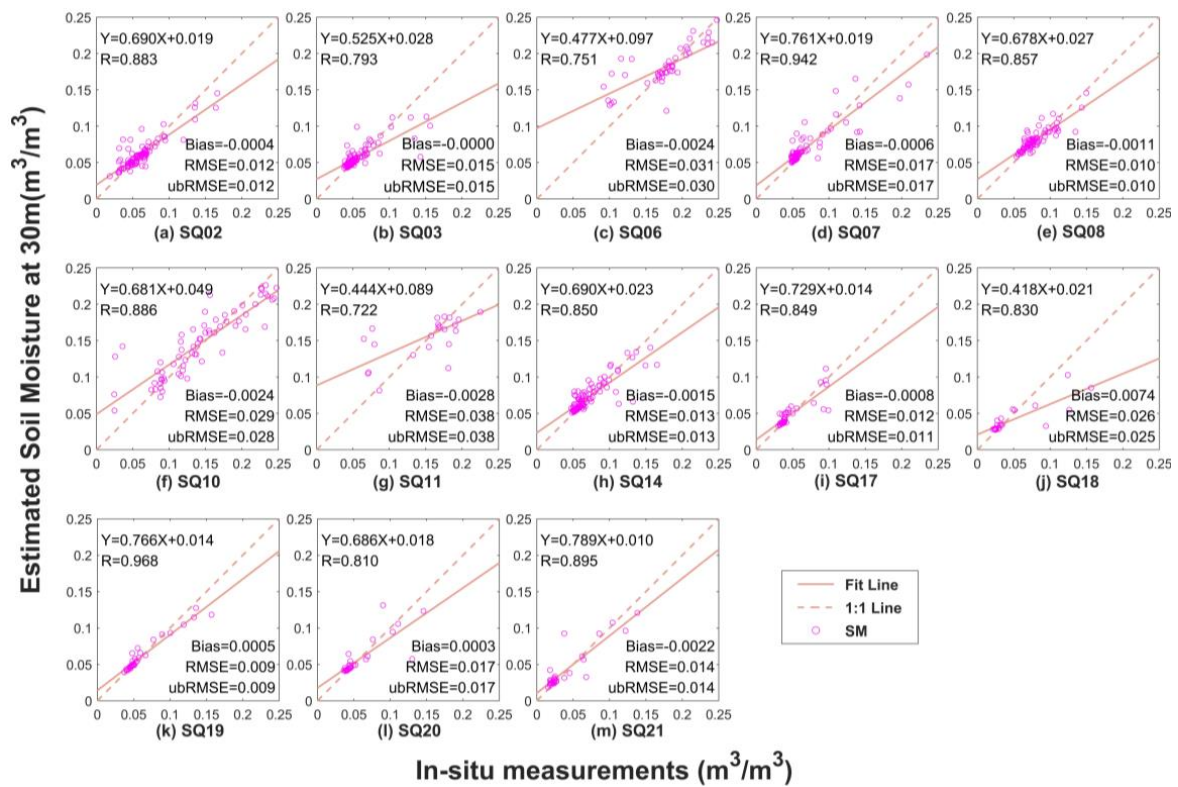
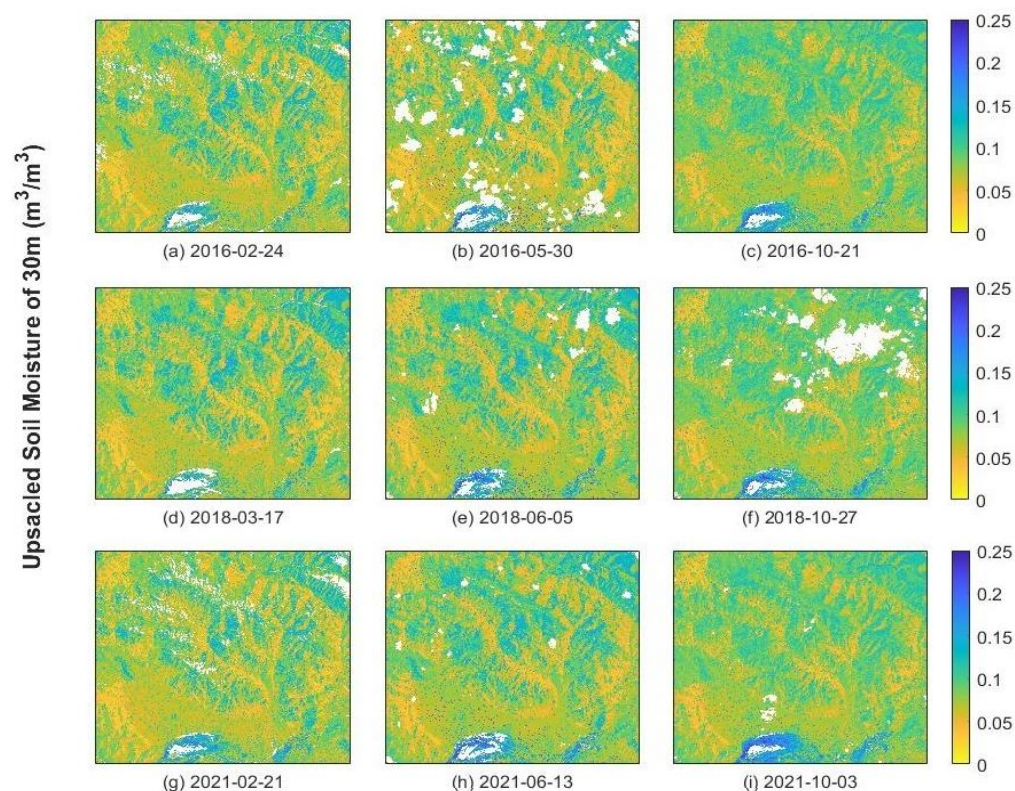


Figure 4. Scatter plot between in situ measurements and 30 m soil moisture estimates based on the RFR upscaling model, with subfigures correspond to 13 soil moisture sites.



**Figure 5.** Estimated soil moisture at 30 m resolution (results from 9 dates were randomly selected for display in the subfigures).

Figure 6 shows the upscaled soil moisture at the 9 km scale, which was obtained by averaging the 30 m soil moisture according to the extent of the SMAP 9 km EASE-2 grid. It is worth mentioning that if more than half of the 90,000 small 30 m grids corresponding to a single 9 km grid contain clouds, the average soil moisture value of the grid will be regarded as invalid data and will not be used for the evaluation of SMAP products.

The upscaling method proposed in this paper was applied to the remote sensing data from March 2013 to December 2021. It can complete the soil moisture time series when the ground observations are missing, so as to realize the long-term time series validation of SMAP products.

#### 4.3. Validation of SMAP SM Products

Based on the upscaled soil moisture at the 9 km scale, we evaluated the SPL3SMP\_E, which is the SMAP global daily 9 km composite radiometer soil moisture product. Figure 7 shows the overall validation results of the SPL3SMP\_E products in Ngari. If the upscaled soil moisture is regarded as the ground truth, the *ubRMSE* and *RMSE* of the L3\_SM\_PE products in the Ngari are  $0.023 \text{ m}^3/\text{m}^3$  and  $0.031 \text{ m}^3/\text{m}^3$ , respectively, meeting the scientific observation requirements of the SMAP satellite mission ( $0.04 \text{ m}^3/\text{m}^3$ ). In addition, the bias is  $0.0205 \text{ m}^3/\text{m}^3$ , indicating that the SPL3SMP\_E products underestimate the soil moisture in Nagri.

Table 2 shows the refined analysis results for 20 grids of SPL3SMP\_E products in the study area (the grid numbers are shown in Figure 1). It was found that the *ubRMSE* and *RMSE* of each grid are within  $0.04 \text{ m}^3/\text{m}^3$ , meeting the SMAP's scientific observation requirements. In particular, all *ubRMSE* values are lower than  $0.026 \text{ m}^3/\text{m}^3$ , indicating that the satellite products have good observation accuracy. All the biases are positive, except for grid 16, meaning that the satellite products universally underestimated the soil moisture of the study area. Additionally, most of the correlations (*R*) are significant at the 0.05–0.07 level.

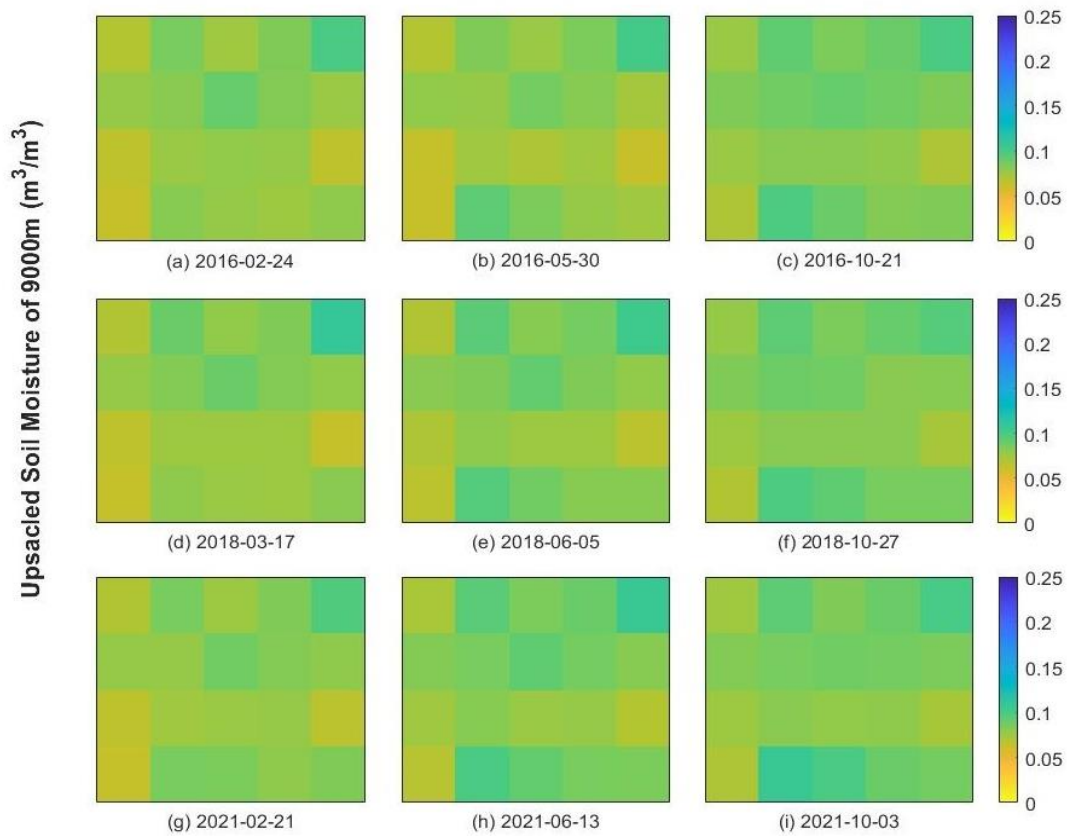


**Figure 6.** Upscaled soil moisture at 9 km resolution (the dates of the subfigures correspond to Figure 5).

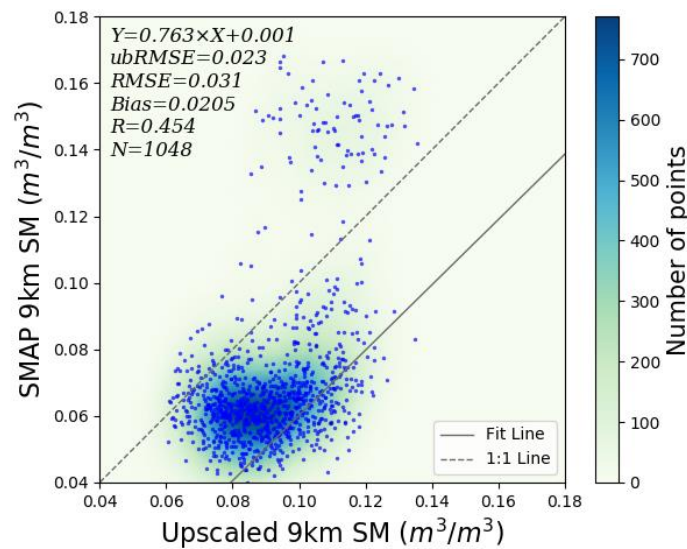


**Figure 7.** The comparison of 9 km upscaled soil moisture data with SMAP soil moisture.

**Table 2.** Evaluation metrics between the 9 km upscaled soil moisture data and the SMAP SM product.

Grid	<i>ubRMSE</i> (m <sup>3</sup> /m <sup>3</sup> )	<i>RMSE</i> (m <sup>3</sup> /m <sup>3</sup> )	<i>Bias</i> (m <sup>3</sup> /m <sup>3</sup> )	<i>R</i>
1	0.0156	0.0234	0.0175	0.4757
2	0.0185	0.0381	0.0333	0.4980
3	0.0177	0.0272	0.0207	0.5796
4	0.0180	0.0260	0.0188	0.6309

**Table 2.** Cont.

Grid	<i>ubRMSE</i> (m <sup>3</sup> /m <sup>3</sup> )	<i>RMSE</i> (m <sup>3</sup> /m <sup>3</sup> )	<i>Bias</i> (m <sup>3</sup> /m <sup>3</sup> )	<i>R</i>
5	0.0180	0.0314	0.0257	0.6253
6	0.0219	0.0320	0.0234	0.4303
7	0.0183	0.0353	0.0302	0.5619
8	0.0176	0.0387	0.0344	0.5363
9	0.0176	0.0329	0.0279	0.5084
10	0.0211	0.0269	0.0167	0.5766
11	0.0200	0.0228	0.0109	0.5460
12	0.0238	0.0286	0.0159	0.6779
13	0.0236	0.0300	0.0185	0.5708
14	0.0251	0.0300	0.0165	0.5531
15	0.0230	0.0240	0.0068	0.5602
16	0.0190	0.0195	−0.0040	0.6380
17	0.0213	0.0390	0.0326	0.6336
18	0.0230	0.0368	0.0288	0.5737
19	0.0203	0.0289	0.0206	0.5872
20	0.0220	0.0297	0.0199	0.5414

Figure 8 plots the time series of 9 km upscaled soil moisture data and satellite-observed soil moisture in six randomly selected grids. In order to ensure the time consistency of data, the upscaled soil moisture and the validated SMAP were both chosen twice a month, corresponding to Landsat’s visit time. It is clear that the SMAP observations in Figure 8 are discontinuous. This is because the soil in Ngari is either covered with snow or frozen from November to May every year, and during this period, the SM data are masked in the SMAP products due to uncertainties in the reference freeze/thaw conditions of satellite retrieval. Nonetheless, we can find that the available valid satellite soil moisture data show distinct seasonality, being high in summer and low in winter, which is consistent with the actual conditions of Ngari. Moreover, it is found that SPL3SMP\_E products overestimate the soil moisture of the Ngari network during the wet period and underestimate it during the dry season. Unfortunately, due to the short duration of the radar operation, it is hard to compare the soil moisture products observed by the radar with the soil moisture products obtained by interpolation.

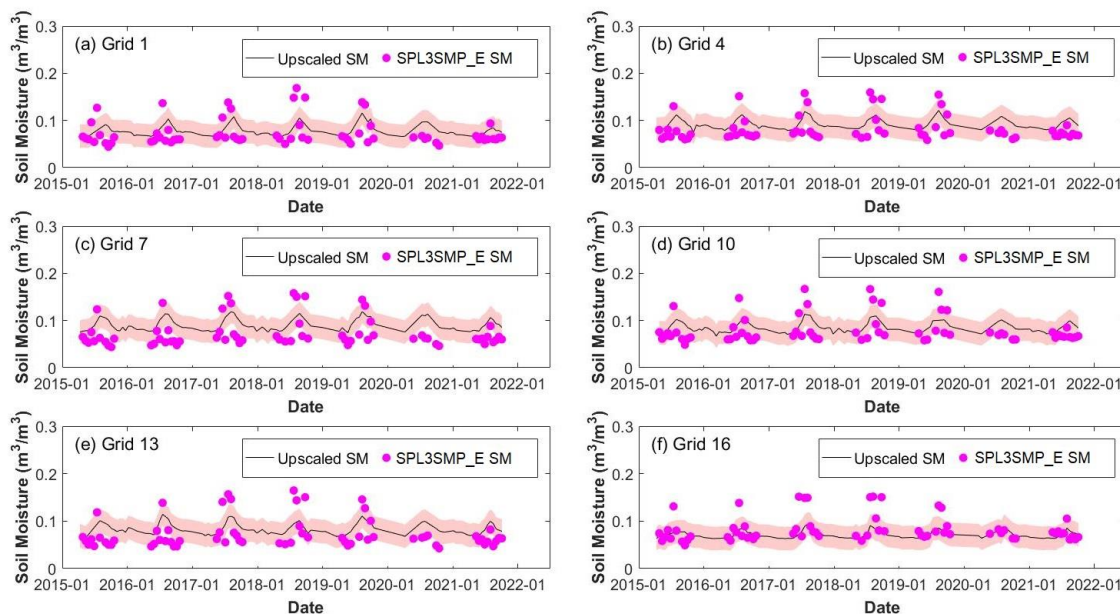


**Figure 8.** Time series comparisons of 9 km upscaled soil moisture data with SMAP soil moisture from April 2015 to December 2021 (6 grids were randomly selected for display in the subfigures).

## 5. Discussion

In order to ensure the effectiveness of satellite SM product validation based on sparse observations, a method is proposed to scale up the in situ measurements to a high-resolution pixel scale (30 m) and then to a coarse grid scale (9 km) using the RFR algorithm. The pixels at the 30 m scale are relatively pure, and, therefore, the spatial representativeness of the satellite observations and in situ measurements are similar. Additionally, the spatial continuity of satellite images can effectively capture the spatial distribution of SM within 9000 m, making up for the limited number and uneven spatial distribution of sparse network sites. Moreover, when ground observations are missing, the long-term historical data from Landsat fill in the gaps caused by the discontinuity in in situ SM and complete the soil moisture time series. In conclusion, it is beneficial to acquire representative soil moisture at the coarse grid scale by using high-resolution remote sensing data as a scale conversion bridge [53].

To accurately simulate the complex relationship between in situ measurements and multi-source auxiliary data, the RFR algorithm was used to construct the upscaling model. Validation and comparison experiments show that the RFR algorithm has ideal upscaling performance, which is superior to the other four upscaling algorithms: GBRT, AdaBoost, RR, and ARD. The poor performance of the RR and ARD algorithms may be due to the fact that they are more suitable for simulating relationships with fewer categories of data.

When we analyze the features of soil moisture, we find that SM has a clear seasonal characteristic, and shows a relatively stable pattern of change over time throughout the year. Typically, soil moisture reaches its lowest level in winter, gradually rises in spring, reaches its peak in summer, and then falls back in autumn (Figure 9). Considering the soil moisture change law over time, this paper incorporates the month information as a feature of soil moisture estimation into the upscale experiment for the first time.

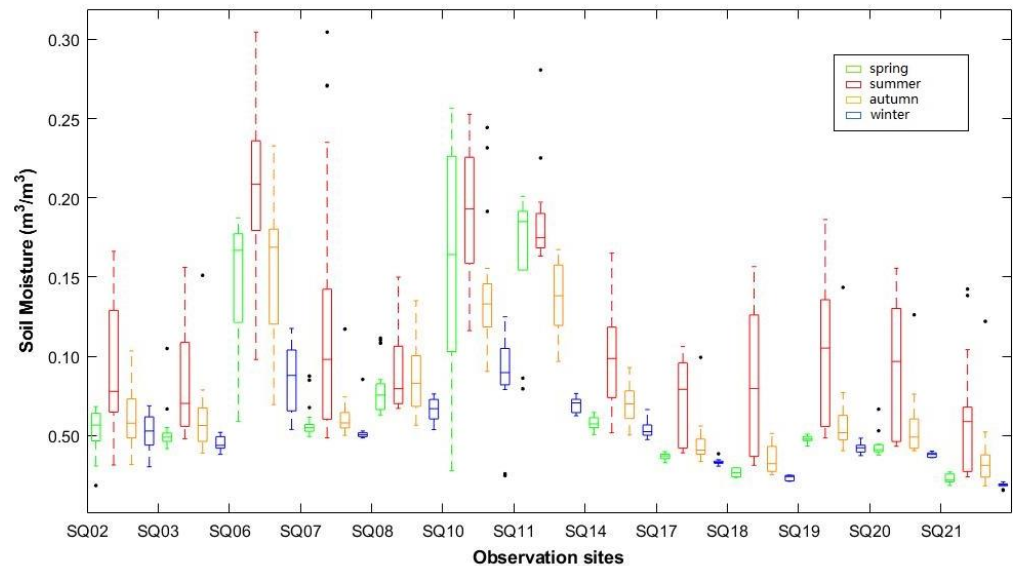


**Figure 9.** Comparison of soil moisture observations in different seasons. The black dots in the box plot represent outliers in the original in-situ measurements.

Figure 10 shows the difference in upscaling model performance with and without month information. It is obvious that the accuracy of the RFR, GBRT, and AdaBoost models is improved when including the month information, with their *ubRMSE* and *RMSE* values decreasing and their *R* values increasing. This suggests that monthly information is actually useful for estimating soil moisture. However, for the RR and ARD algorithms, the accuracy of soil moisture estimation decreased after using monthly information. This might be due to the fact that adding the monthly information makes the dataset larger and the relationships between the data more complicated, making it harder for the RR and ARD

algorithms to simulate the relationships, and producing unfavorable results. It reminds us that the usage of auxiliary data may not always have beneficial impacts and that while building an upscaling model, the suitability of data and algorithm should be taken into consideration. It is also important to note that the RFR algorithm shows a strong ability to deal with complex nonlinear relations in the experiment and is a good choice for modeling multi-source data and in situ measurements.

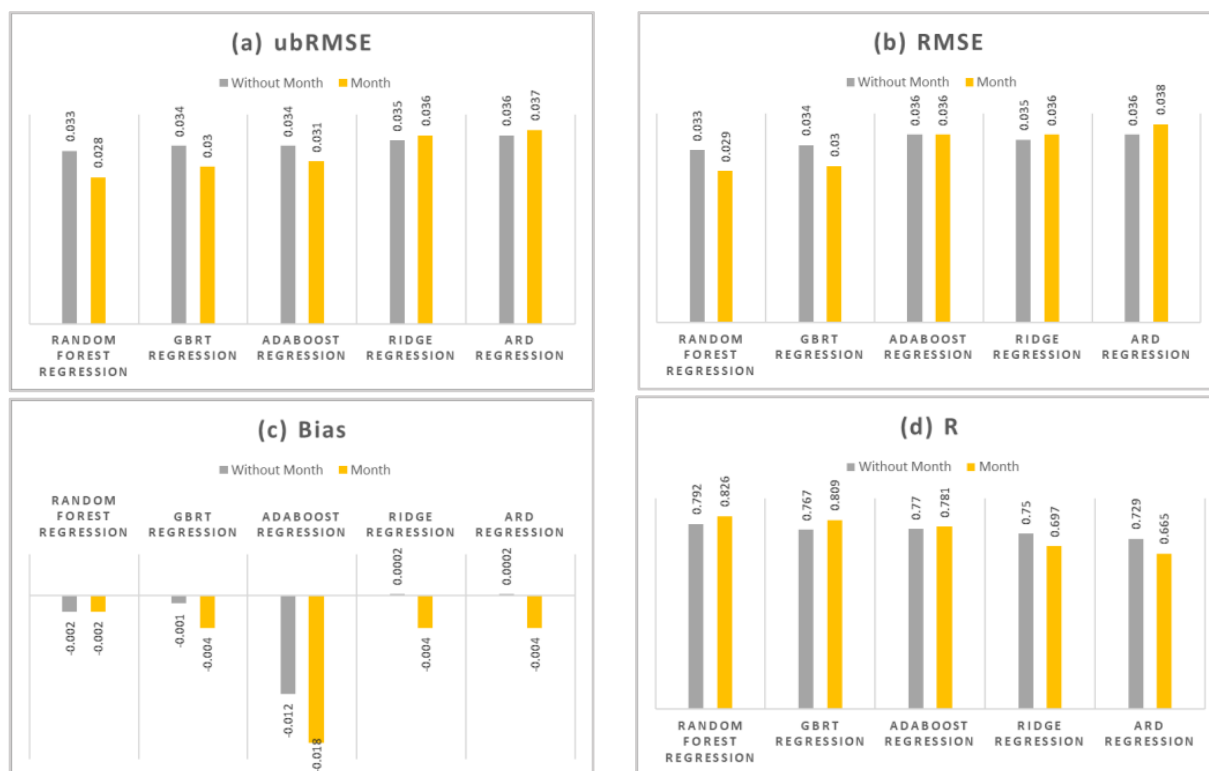


**Figure 10.** Comparison of the performance of 5 upscaling algorithms with and without monthly information with metric indicators (a) *ubRMSE*, (b) *RMSE*, (c) *bias* and (d) *R*.

To ensure the reliability of SMAP product validation, a long time series of upscaled SM was obtained based on the proposed method. The validation results demonstrate that the SPL3SMP\_E products satisfy the requirements of their scientific goal. However, we found that the products underestimate the actual soil moisture in the Ngari area which may be related to the field environment and the properties of the radiometer itself. Sadly, SMAP's radar malfunctioned in April 2015, which prevents us from conducting further comparisons and analyses.

## 6. Conclusions

In this paper, a soil-moisture-upscaling model suitable for sparse ground-based soil moisture observations was constructed to evaluate SMAP products on the Qinghai–Tibet Plateau. The model utilized machine learning algorithms to effectively capture the complex relationship between in situ measurements and multi-source high-resolution remote sensing auxiliary information. The inclusion of remote sensing auxiliary information compensated for the limited number of sparse ground observation sites and enabled the acquisition of spatially representative large-scale soil moisture reference values, which were then used for the evaluation of SMAP products.

We explored five machine learning algorithms for upscaling. The experimental results demonstrated that the random forest regression (RFR) algorithm was a good choice for constructing complex upscaling models, outperforming the gradient boosting regression tree (GBRT), AdaBoost, ridge regression (RR), and automatic relevance determination (ARD) models. We also explored the potential of different auxiliary data in obtaining reliable

estimates of soil moisture and found that, in addition to known soil-moisture-related features, the month information was an effective variable for estimating soil moisture.

Based on the upscaled soil moisture, the long-term SPL3SMP\_E products in the Ngari region since the launch of the SMAP mission were evaluated. The results showed that (1) Ngari's SPL3SMP\_E products contain a large amount of invalid data from November to May due to uncertainties in the satellite retrieval of SM during the frozen season; (2) whether in the entire study area or in a single grid, the  $ubRMSE$  is within  $0.04 \text{ m}^3/\text{m}^3$ , meeting the scientific observation requirements of the SMAP mission; and (3) SPL3SMP\_E products underestimate the soil moisture in Ngari as a whole, but often overestimate the soil moisture during the wet period. Future work will focus on improving the performance of upscaling methods and expanding their application to other regions.

**Author Contributions:** Conceptualization, Jia Chen, Fengmin Hu and Changqing Huang; methodology, Jia Chen and Fengmin Hu; software, Jia Chen, Fengmin Hu and Junjie Li; validation, Jia Chen and Fengmin Hu; formal analysis, Jia Chen, Fengmin Hu and Yijia Xie; investigation, Jia Chen, Fengmin Hu and Wen Zhang; resources, Jia Chen and Fengmin Hu; data curation, Jia Chen, Fengmin Hu and Yijia Xie; writing—original draft preparation, Jia Chen; writing—review and editing, Jia Chen, Fengmin Hu, Junjie Li, Wen Zhang and Lingkui Meng; visualization, Jia Chen, Fengmin Hu and Yijia Xie; supervision, Wen Zhang, Changqing Huang and Lingkui Meng; project administration, Wen Zhang, Changqing Huang and Lingkui Meng; funding acquisition, Lingkui Meng. All authors have read and agreed to the published version of the manuscript.

**Funding:** This research was funded by the National Key Research and Development Program of China (No.2021YFB3900603).

**Data Availability Statement:** Publicly available data used to support the findings of this study can be found at following links: SMAP: <https://smap.jpl.nasa.gov/nasa.gov>, accessed on 17 February 2022; Ngari in situ observations: <https://data.tpdc.ac.cn/home>, accessed on 18 February 2022; Landsat 8: <https://landsat.gsfc.nasa.gov/>, accessed on 22 February 2022; ASTER GDEM: <https://asterweb.jpl.nasa.gov/>, accessed on 21 March 2022; GlobeLand30: <http://globeland30.org/>, accessed on 21 March 2022.

**Acknowledgments:** The authors would like to thank the editors and reviewers for their valuable reviews and suggestions.

**Conflicts of Interest:** The authors declare no conflict of interest.

## References

- Al-Yaari, A.; Wigneron, J.-P.; Kerr, Y.; Rodriguez-Fernandez, N.; O'Neill, P.; Jackson, T.; De Lannoy, G.; Al Bitar, A.; Mialon, A.; Richaume, P.; et al. Evaluating soil moisture retrievals from ESA's SMOS and NASA's SMAP brightness temperature datasets. *Remote Sens. Environ.* **2017**, *193*, 257–273. [CrossRef] [PubMed]
- Zhao, T.; Shi, J.; Lv, L.; Xu, H.; Chen, D.; Cui, Q.; Jackson, T.J.; Yan, G.; Jia, L.; Chen, L.; et al. Soil moisture experiment in the Luan River supporting new satellite mission opportunities. *Remote Sens. Environ.* **2020**, *240*, 111680. [CrossRef]
- Hu, F.; Wei, Z.; Yang, X.; Xie, W.; Li, Y.; Cui, C.; Yang, B.; Tao, C.; Zhang, W.; Meng, L. Assessment of SMAP and SMOS soil moisture products using triple collocation method over Inner Mongolia. *J. Hydrol. Reg. Stud.* **2022**, *40*, 101027. [CrossRef]
- Xing, Z.; Fan, L.; Zhao, L.; De Lannoy, G.; Frappart, F.; Peng, J.; Li, X.; Zeng, J.; Al-Yaari, A.; Yang, K.; et al. A first assessment of satellite and reanalysis estimates of surface and root-zone soil moisture over the permafrost region of Qinghai-Tibet Plateau. *Remote Sens. Environ.* **2021**, *265*, 112666. [CrossRef]
- Zeng, J.; Li, Z.; Chen, Q.; Bi, H.; Qiu, J.; Zou, P. Evaluation of remotely sensed and reanalysis soil moisture products over the Tibetan Plateau using in-situ observations. *Remote Sens. Environ.* **2015**, *163*, 91–110. [CrossRef]
- Zhao, W.; Sánchez, N.; Lu, H.; Li, A. A spatial downscaling approach for the SMAP passive surface soil moisture product using random forest regression. *J. Hydrol.* **2018**, *563*, 1009–1024. [CrossRef]
- Bogena, H.; Herbst, M.; Huisman, J.; Rosenbaum, U.; Weuthen, A.; Vereecken, H. Potential of Wireless Sensor Networks for Measuring Soil Water Content Variability. *Vadose Zone J.* **2010**, *9*, 1002–1013. [CrossRef]
- Brocca, L.; Ciabatta, L.; Massari, C.; Camici, S.; Tarpanelli, A. Soil Moisture for Hydrological Applications: Open Questions and New Opportunities. *Water* **2017**, *9*, 140. [CrossRef]
- Li, X.; Wigneron, J.-P.; Fan, L.; Frappart, F.; Yueh, S.H.; Colliander, A.; Ebtehaj, A.; Gao, L.; Fernandez-Moran, R.; Liu, X.; et al. A new SMAP soil moisture and vegetation optical depth product (SMAP-IB): Algorithm, assessment and inter-comparison. *Remote Sens. Environ.* **2022**, *271*, 112921. [CrossRef]

10. Ye, N.; Walker, J.P.; Wu, X.; de Jeu, R.; Gao, Y.; Jackson, T.J.; Jonard, F.; Kim, E.; Merlin, O.; Pauwels, V.R.N.; et al. The Soil Moisture Active Passive Experiments: Validation of the SMAP Products in Australia. *IEEE Trans. Geosci. Remote Sens.* **2020**, *59*, 2922–2939. [[CrossRef](#)]
11. Ma, H.; Zeng, J.; Chen, N.; Zhang, X.; Cosh, M.H.; Wang, W. Satellite surface soil moisture from SMAP, SMOS, AMSR2 and ESA CCI: A comprehensive assessment using global ground-based observations. *Remote Sens. Environ.* **2019**, *231*, 111215. [[CrossRef](#)]
12. Ming, W.; Ji, X.; Zhang, M.; Li, Y.; Liu, C.; Wang, Y.; Li, J. A Hybrid Triple Collocation-Deep Learning Approach for Improving Soil Moisture Estimation from Satellite and Model-Based Data. *Remote Sens.* **2022**, *14*, 1744. [[CrossRef](#)]
13. Qin, J.; Zhao, L.; Chen, Y.; Yang, K.; Yang, Y.; Chen, Z.; Lu, H. Inter-comparison of spatial upscaling methods for evaluation of satellite-based soil moisture. *J. Hydrol.* **2015**, *523*, 170–178. [[CrossRef](#)]
14. Zheng, J.; Zhao, T.; Lü, H.; Shi, J.; Cosh, M.H.; Ji, D.; Jiang, L.; Cui, Q.; Lu, H.; Yang, K.; et al. Assessment of 24 soil moisture datasets using a new in situ network in the Shandian River Basin of China. *Remote Sens. Environ.* **2022**, *271*, 112891. [[CrossRef](#)]
15. Crow, W.T.; Berg, A.A.; Cosh, M.H.; Loew, A.; Mohanty, B.P.; Panciera, R.; de Rosnay, P.; Ryu, D.; Walker, J.P. Upscaling sparse ground-based soil moisture observations for the validation of coarse-resolution satellite soil moisture products. *Rev. Geophys.* **2012**, *50*, 2. [[CrossRef](#)]
16. Zeng, J.; Chen, K.-S.; Bi, H.; Chen, Q. A Preliminary Evaluation of the SMAP Radiometer Soil Moisture Product Over United States and Europe Using Ground-Based Measurements. *IEEE Trans. Geosci. Remote Sens.* **2016**, *54*, 4929–4940. [[CrossRef](#)]
17. Ma, C.; Li, X.; Wei, L.; Wang, W. Multi-Scale Validation of SMAP Soil Moisture Products over Cold and Arid Regions in Northwestern China Using Distributed Ground Observation Data. *Remote Sens.* **2017**, *9*, 327. [[CrossRef](#)]
18. Wang, J.; Ge, Y.; Heuvelink, G.B.M.; Zhou, C. Upscaling In Situ Soil Moisture Observations to Pixel Averages with Spatio-Temporal Geostatistics. *Remote Sens.* **2015**, *7*, 11372–11388. [[CrossRef](#)]
19. Zhang, J.; Li, X.; Yang, R.; Liu, Q.; Zhao, L.; Dou, B. An Extended Kriging Method to Interpolate Near-Surface Soil Moisture Data Measured by Wireless Sensor Networks. *Sensors* **2017**, *17*, 1390. [[CrossRef](#)]
20. Cai, X.; Pan, M.; Chaney, N.W.; Colliander, A.; Misra, S.; Cosh, M.H.; Crow, W.T.; Jackson, T.J.; Wood, E.F. Validation of SMAP soil moisture for the SMAPVEX15 field campaign using a hyper-resolution model. *Water Resour. Res.* **2017**, *53*, 3013–3028. [[CrossRef](#)]
21. Chen, Y.; Yuan, H. Evaluation of nine sub-daily soil moisture model products over China using high-resolution in situ observations. *J. Hydrol.* **2020**, *588*, 125054. [[CrossRef](#)]
22. Crow, W.T.; Ryu, D.; Famiglietti, J.S. Upscaling of field-scale soil moisture measurements using distributed land surface modeling. *Adv. Water Resour.* **2005**, *28*, 1–14. [[CrossRef](#)]
23. Pan, M.; Cai, X.; Chaney, N.W.; Entekhabi, D.; Wood, E.F. An initial assessment of SMAP soil moisture retrievals using high-resolution model simulations and in situ observations. *Geophys. Res. Lett.* **2016**, *43*, 9662–9668. [[CrossRef](#)]
24. Qin, J.; Yang, K.; Lu, N.; Chen, Y.; Zhao, L.; Han, M. Spatial upscaling of in-situ soil moisture measurements based on MODIS-derived apparent thermal inertia. *Remote Sens. Environ.* **2013**, *138*, 1–9. [[CrossRef](#)]
25. Spennemann, P.; Fernández-Long, M.; Gattinoni, N.; Cammalleri, C.; Naumann, G. Soil moisture evaluation over the Argentine Pampas using models, satellite estimations and in-situ measurements. *J. Hydrol. Reg. Stud.* **2020**, *31*, 100723. [[CrossRef](#)]
26. Kang, J.; Jin, R.; Li, X.; Zhang, Y.; Zhu, Z. Spatial Upscaling of Sparse Soil Moisture Observations Based on Ridge Regression. *Remote Sens.* **2018**, *10*, 192. [[CrossRef](#)]
27. Mardan, M.; Ahmadi, S. Soil moisture retrieval over agricultural fields through integration of synthetic aperture radar and optical images. *GIScience Remote Sens.* **2021**, *58*, 1276–1299. [[CrossRef](#)]
28. Zhang, Y.; Liang, S.; Zhu, Z.; Ma, H.; He, T. Soil moisture content retrieval from Landsat 8 data using ensemble learning. *ISPRS J. Photogramm. Remote Sens.* **2022**, *185*, 32–47. [[CrossRef](#)]
29. Zhang, D.; Zhang, W.; Huang, W.; Hong, Z.; Meng, L. Upscaling of Surface Soil Moisture Using a Deep Learning Model with VIIRS RDR. *ISPRS Int. J. Geo-Inf.* **2017**, *6*, 130. [[CrossRef](#)]
30. Clewley, D.; Whitcomb, J.B.; Akbar, R.; Silva, A.R.; Berg, A.; Adams, J.R.; Caldwell, T.; Entekhabi, D.; Moghaddam, M. A Method for Upscaling In Situ Soil Moisture Measurements to Satellite Footprint Scale Using Random Forests. *IEEE J. Sel. Top. Appl. Earth Obs. Remote Sens.* **2017**, *10*, 2663–2673. [[CrossRef](#)]
31. Entekhabi, D.; Njoku, E.G.; O'Neill, P.E.; Kellogg, K.H.; Crow, W.T.; Edelstein, W.N.; Entin, J.K.; Goodman, S.D.; Jackson, T.J.; Johnson, J.; et al. The Soil Moisture Active Passive (SMAP) Mission. *Proc. IEEE* **2010**, *98*, 704–716. [[CrossRef](#)]
32. Chan, S.; Bindlish, R.; O'Neill, P.; Jackson, T.; Njoku, E.; Dunbar, S.; Chaubell, J.; Piepmeier, J.; Yueh, S.; Entekhabi, D.; et al. Development and assessment of the SMAP enhanced passive soil moisture product. *Remote Sens. Environ.* **2017**, *204*, 931–941. [[CrossRef](#)]
33. Chen, Q.; Zeng, J.; Cui, C.; Li, Z.; Chen, K.-S.; Bai, X.; Xu, J. Soil Moisture Retrieval From SMAP: A Validation and Error Analysis Study Using Ground-Based Observations Over the Little Washita Watershed. *IEEE Trans. Geosci. Remote Sens.* **2017**, *56*, 1394–1408. [[CrossRef](#)]
34. Zhang, X.; Zhang, T.; Zhou, P.; Shao, Y.; Gao, S. Validation Analysis of SMAP and AMSR2 Soil Moisture Products over the United States Using Ground-Based Measurements. *Remote Sens.* **2017**, *9*, 104. [[CrossRef](#)]
35. Colliander, A.; Reichle, R.H.; Crow, W.T.; Cosh, M.H.; Chen, F.; Chan, S.; Das, N.N.; Bindlish, R.; Chaubell, J.; Kim, S.; et al. Validation of Soil Moisture Data Products from the NASA SMAP Mission. *IEEE J. Sel. Top. Appl. Earth Obs. Remote Sens.* **2021**, *15*, 364–392. [[CrossRef](#)]

36. Chen, Y.; Yang, K.; Qin, J.; Cui, Q.; Lu, H.; La, Z.; Han, M.; Tang, W. Evaluation of SMAP, SMOS, and AMSR2 soil moisture retrievals against observations from two networks on the Tibetan Plateau. *J. Geophys. Res. Atmos.* **2017**, *122*, 5780–5792. [[CrossRef](#)]
37. Yao, T.; Wu, G.; Xu, B.; Wang, W.; Gao, J.; An, B. Asian water tower change and its impacts. *Bull. Chin. Acad. Sci.* **2019**, *34*, 1203–1209.
38. Zhang, Q.; Fan, K.; Singh, V.P.; Sun, P.; Shi, P. Evaluation of Remotely Sensed and Reanalysis Soil Moisture Against In Situ Observations on the Himalayan-Tibetan Plateau. *J. Geophys. Res. Atmos.* **2018**, *123*, 7132–7148. [[CrossRef](#)]
39. Liu, J.; Chai, L.; Lu, Z.; Qu, Y.; Wang, J.; Yang, S. Validation of Five Passive Microwave Remotely Sensed Soil Moisture Products over the Qinghai-Tibet Plateau, China. In Proceedings of the IGARSS 2019—2019 IEEE International Geoscience and Remote Sensing Symposium, Yokohama, Japan, 28 July 2019–2 August 2019; pp. 6182–6185. [[CrossRef](#)]
40. Yang, K.; Wu, H.; Qin, J.; Lin, C.; Tang, W.; Chen, Y. Recent climate changes over the Tibetan Plateau and their impacts on energy and water cycle: A review. *Glob. Planet. Chang.* **2014**, *112*, 79–91. [[CrossRef](#)]
41. Wang, X.; Lü, H.; Crow, W.T.; Zhu, Y.; Wang, Q.; Su, J.; Zheng, J.; Gou, Q. Assessment of SMOS and SMAP soil moisture products against new estimates combining physical model, a statistical model, and in-situ observations: A case study over the Huai River Basin, China. *J. Hydrol.* **2021**, *598*, 126468. [[CrossRef](#)]
42. Wei, Z.; Meng, Y.; Zhang, W.; Peng, J.; Meng, L. Downscaling SMAP soil moisture estimation with gradient boosting decision tree regression over the Tibetan Plateau. *Remote Sens. Environ.* **2019**, *225*, 30–44. [[CrossRef](#)]
43. Su, Z.; Wen, J.; Dente, L.; van der Velde, R.; Wang, L.; Ma, Y.; Yang, K.; Hu, Z. The Tibetan Plateau observatory of plateau scale soil moisture and soil temperature (Tibet-Obs) for quantifying uncertainties in coarse resolution satellite and model products. *Hydrol. Earth Syst. Sci.* **2011**, *15*, 2303–2316. [[CrossRef](#)]
44. Kang, J.; Jin, R.; Li, X. Regression Kriging-Based Upscaling of Soil Moisture Measurements from a Wireless Sensor Network and Multiresource Remote Sensing Information Over Heterogeneous Cropland. *IEEE Geosci. Remote Sens. Lett.* **2014**, *12*, 92–96. [[CrossRef](#)]
45. Breiman, L. Random forests. *Mach. Learn.* **2001**, *45*, 5–32. [[CrossRef](#)]
46. Friedman, J.H. Greedy function approximation: A gradient boosting machine. *Ann. Stat.* **2001**, *29*, 1189–1232. [[CrossRef](#)]
47. Freund, Y.; Schapire, R.E. A Decision-Theoretic Generalization of On-Line Learning and an Application to Boosting. *J. Comput. Syst. Sci.* **1997**, *55*, 119–139. [[CrossRef](#)]
48. Hoerl, A.E.; Kennard, R.W. Ridge Regression: Applications to Nonorthogonal Problems. *Technometrics* **1970**, *12*, 69–82. [[CrossRef](#)]
49. Reichstein, M.; Camps-Valls, G.; Stevens, B.; Jung, M.; Denzler, J.; Carvalhais, N.; Prabhat. Deep learning and process understanding for data-driven Earth system science. *Nature* **2019**, *566*, 195–204. [[CrossRef](#)] [[PubMed](#)]
50. Yuan, Q.; Shen, H.; Li, T.; Li, Z.; Li, S.; Jiang, Y.; Xu, H.; Tan, W.; Yang, Q.; Wang, J.; et al. Deep learning in environmental remote sensing: Achievements and challenges. *Remote Sens. Environ.* **2020**, *241*, 111716. [[CrossRef](#)]
51. Entekhabi, D.; Reichle, R.H.; Koster, R.D.; Crow, W.T. Performance Metrics for Soil Moisture Retrievals and Application Requirements. *J. Hydrometeorol.* **2010**, *11*, 832–840. [[CrossRef](#)]
52. Liu, Y.; Zhou, Y.; Lu, N.; Tang, R.; Liu, N.; Li, Y.; Yang, J.; Jing, W.; Zhou, C. Comprehensive assessment of Fengyun-3 satellites derived soil moisture with in-situ measurements across the globe. *J. Hydrol.* **2021**, *594*, 125949. [[CrossRef](#)]
53. Zhao, W.; Sanchez, N.; Li, A. Triangle Space-Based Surface Soil Moisture Estimation by the Synergistic Use of In Situ Measurements and Optical/Thermal Infrared Remote Sensing: An Alternative to Conventional Validations. *IEEE Trans. Geosci. Remote Sens.* **2018**, *56*, 4546–4558. [[CrossRef](#)]

**Disclaimer/Publisher’s Note:** The statements, opinions and data contained in all publications are solely those of the individual author(s) and contributor(s) and not of MDPI and/or the editor(s). MDPI and/or the editor(s) disclaim responsibility for any injury to people or property resulting from any ideas, methods, instructions or products referred to in the content.